

## Experimental Investigation of 150 mm Diameter Large Hybrid Foil/Magnetic Bearing

Hooshang Heshmat and David S. Xu

Mohawk Innovative Technology, Inc.  
1037 Watervliet-Shaker Rd. Albany NY 12205, USA  
Phone: (518)862-4290, Fax: (518)862-4293, E-mail: [hheshmat@miti.cc](mailto:hheshmat@miti.cc), [dsxu@miti.cc](mailto:dsxu@miti.cc)

### ABSTRACT

By combining both compliant foil bearing (CFB) and active magnetic bearing (AMB) advantages, the hybrid foil/magnetic bearing (HFMB) can obtain high load capacity at all speeds.

A brief overview of a universal test rig with the largest 150 mm HFMB is presented. Experimental investigation was performed in different modes by means of switching AMB on or off: AMB mode at low speed, CFB mode at high speed, hybrid mode with AMB as a bearing and hybrid mode with AMB as a loader. Data from a series of rotor-bearing system tests are presented. Having recently made efforts to complete the HFMB test (side-by-side), the largest 150 mm CFB passed through its first (3,820 rpm) and second (11,770 rpm) critical speed and reached 26,923 rpm (i.e. 4 MDN). On the other extreme side, the 150 mm CFB testing has shown that it can bear as low as 645 rpm without shaft/foil touch, high temperature rise and large motor torque increases. That means the lift off or touch down speed is very low with a surface velocity  $U$  of less than 5 m/s. The coating used on the foil was Korolon 800 and the rotor surface was electrolyzed.

Transient tests, simulating magnetic bearing failures at speeds as low as 700rpm were also completed. It is shown that CFB has the ability to be a reliable auxiliary/backup bearing for the magnetic bearing system.

This  $\phi 150$ mm foil bearing is sized to meet a wide range of potential applications such as gas turbine engines for high-performance commercial and general aviation aircraft systems as well as larger industrial compressors.

### INTRODUCTION

To address the demands of highly competitive industries such as aerospace and power propulsion, efficient and reliable turbomachines are required. These demands include higher operating speeds and higher temperatures. In the near future, advanced turbomachinery is expected to require bearings capable of continuous operation of between 3 to 4 million DN (where  $D$  is the diameter in mm,  $N$  is the shaft speed in rpm) at temperatures of up to 820°C. That will place severe constraints on existing bearing systems. The current state-of-the-art liquid-lubricated bearing does suffer from temperature limitations, while the rolling element bearing has a limited life at extreme conditions with uncertain dynamic performance. It requires an oil lubrication system as well.

Non-contact bearing systems such as oil-free, high-load CFB, AMB and HFMB might be the better solutions. AMB provides excellent performance at low speeds where CFB has limited load capacity, while CFB provides excellent performance at high speed where AMB has transient shock and failure mode limitations. A HFMB combines those two advantages and compensates for each

bearing's limitations, therefore, providing a high load capacity at all speeds [1-13]. Such a hybrid HFMB also has many other merits. For instance, unlike more conventional magnetic bearing applications, the HFMB does not require a separate auxiliary/backup bearing for protection. In case of AMB failure, CFB acts as a backup bearing. The development of the HFMB will have additional significant military and commercial potential in aircraft/marine gas turbine engines, pipeline compressors and pumps, auxiliary power units, flywheel energy storage devices and other high speed rotating machinery.

There are two configurations of the HFMB: (1) AMB and CFB in side-by-side configuration and (2) AMB and CFB in nested configuration. There is the axial space limitation of HFMB with side-by-side configuration, but the nested HFMB configuration has radial space limitation and difficulty running at high temperature due to temperature sensitivity of AMB. Several papers which describe the test results of these two kinds of HFMB configurations ( $\phi 100$  mm CFB with  $\phi 121$  mm AMB) have been published [9-13] and a series of tests of CFB from 35 mm to 100 mm diameter have been investigated over the past 20 years [1,6,9-13]. Fig. 1 shows the load capacity for 35 and 100 mm diameter CFBs at room temperature.

With the increasing challenge facing advanced turbomachinery, recent developments in advanced CFBs have begun to address the major limiting factors hindering the use of AMBs and CFBs in the larger regional gas turbine engines, namely the load carrying capacity, shock tolerance, high speed and high temperature operation. The scalability of existing designs (typically 35 mm to 100 mm) to the much larger size (150 mm) required by larger turbomachinery has not been widely addressed. Specially, it is insufficient for the true widespread application of bearing sizes in the range of 140-150 mm in diameter. This additional increase in bearing size poses challenges in reliable experimental data and the manufacturing approaches for CFBs. Additionally, the larger CFB will also require new and innovative designs and manufacturing techniques to address the thermal management of the increasing internal heat generation and the structural stiffness patterns to maintain the desired gas film thickness even in the presence of significantly higher loads and pressures. Thus, while the demonstration of the 100 mm diameter CFB represents a technological breakthrough, much needs to be done in the areas of thermal management, bump foil compliance under very high loads, tribo-materials pairing to accommodate temperatures to 650°C and so on. Therefore, the experimental investigation of the load carrying capacity, high speed and high temperature operation for the large diameter  $\phi 150$  mm CFB is placed on the agenda. In this

paper the experimental investigation and some breakthrough results of the largest foil journal bearing  $\phi 150$  mm CFB are presented.

### EXPERIMENTAL SET-UP

In order to investigate the capability of the largest ( $\phi 150$  mm) foil bearing to meet advanced gas turbine engine needs at high speed (20,000rpm) and high temperature (650<sup>o</sup>C), as shown in Fig.2, an existing test rig[14] was modified. To simulate an engine installation, an approximately 65 kg, 0.85 m long rotor was used. The set up includes a ball bearing (REB), a magnetic bearing (AMB) and a compliant foil bearing (CFB). The REB and CFB are located at the opposite end of the rotor. This allows for easier assembly and disassembly of different kinds of foil bearings with different bearing parameters, materials and coatings. To the best of authors' knowledge, the  $\phi 150$  mm foil bearing used in these tests is believed to be the largest compliant foil journal bearing ever built and tested. As shown in Fig.2, the AMB is set in the middle and can be used as either a support bearing or a loader for exerting load on the CFB. Alignment is very important in the test rig. The rotor is driven with an electrical motor and connected via a coupling. This coupling was axially soft and radially stiff. The drive motor was a three-phase motor with about 44.7 kW of power and a maximum rotational speed 30,000 rpm. An optical speed pick-up was used to obtain rotor speed and as a phase reference. Displacement probes were installed in vertical and horizontal directions close to AMB, CFB and REB for monitoring the rotor orbits. Thermocouples were installed on each bearing. Pressure transducers were also provided to record cooling air pressures. Cooling air flow was recorded with mass air flow sensors. Loading on the CFB with the AMB loader was calibrated to determine actual applied load and monitored by AMB bias currents.

Capabilities of this test rig are as follows:

- $\phi 150$ mm CFB and HFMB bearings with different kinds of configuration, parameters, materials and coatings.
- Rotor speed range 0 ~ 20,000 rpm (up to 30,000 rpm)
- Temperatures up to 816<sup>o</sup>C for the CFB
- Orbit control within  $\pm 0.0002$ "

Two types of rotor (hollow shaft with sleeve and solid shaft) were employed. The hollow shaft was approximately 0.84 m long, 46 kg weight and made of Inconel 718, which is very strong and capable of resisting high temperatures and high stresses. This hollow shaft used a sleeve with  $\phi 150$  mm OD to match the CFB ID. The sleeve was mounted on the rotor with high interference in order to avoid detachment at high speed and high load. A solid shaft with OD at 150 mm for CFB journal was used, which weighed about 65 kg. After final machining and heat treatment, the rotor needed to be electrolyzed for room temperature testing.

The AMB in this test rig was used to provide the following tasks:

- Levitate rotor at zero and low speed during run-up and coast-down course in order to avoid contact, rub and wear between rotor and bearing
- Combine with CFB to support rotor in a hybrid mode
- Orbit control while the rotor is running
- Apply a load to the rotor while the rotor is running on the REB and CFB

The AMB parameters are a hetro-polar magnetic bearing of 8 poles with an air gap 0.508 mm, laminate sheets with 0.19 mm thickness

made of material Hyperco, bias coil current 10A and control coil current 10A for a total of 1,080 amp-turns of the control coils. The force produced by the AMB was 726 kg. The rotor laminations were stacked on a liner, and the liner was then shrink-fitted onto the rotor. Similar laminations were used for the stator.

The testing  $\phi 150$  mm CFB (Fig.3) was conducted to address the following tasks:

- Combine with AMB to support rotor in a hybrid mode with side-by-side HFMB configuration
- Act as an auxiliary/backup bearing of the AMB
- Testing of CFB bearing performance with different parameters (foil thickness, bearing clearance, bump stiffness, etc.), materials and coatings at room temperature or 650<sup>o</sup>C high temperature, and at speed up to 30,000 rpm. The rotor can be running on the REB and CFB with AMB either as a bearing in hybrid mode, or as a loader in the CFB mode alone.

The essential feature of the CFB is its two-fold mechanism of imparting stiffness and damping to the system. One is via the geometry and materials of the compliant support structure, which can consist of corrugated bump foils to provide necessary stiffness and damping. The other is due to the hydrodynamic film between rotor and top foil. In order to measure and monitor the temperature in the foil bearing, several thermocouples were installed in the upstream and downstream sides of the CFB.

Due to the operating conditions of high loads and high speeds, cooling air was used for better temperature distribution and avoiding high temperature spots in the foil bearing. The bulk of the air was blown into the bearing with a certain amount of pressure, passing through the bump foil layer between the top foil and the housing and the clearance between the top foil and the rotor as well.

To prevent the rotor and bearing surfaces from the severe rub and wear during the start up and shut down to a stop, anti-wear coating is very important. In this room temperature test, the foil coating used was Korolon 800 with the rotor surface electrolyzed.

A deep groove ball bearing with 30 mm ID, 62 mm OD and 23.8 mm length was employed in this test rig. The ball bearing housing included a squirrel cage for holding the ball bearing and shear damper that provided structural damping for the ball bearing during the test operation. Two thermocouples were installed on the back of the ball bearing for measuring the temperature.

The displacements of the rotor at different positions (X and Y directions near the AMB, CFB and REB) are measured by means of different sorts of the eddy-current probes. The signals of those probes near AMB are then fed back to the AMB controller system in order to adjust the rotor position. The bearings are controlled by a PC/DSP based system using a modified proportional-integral-derivative (PID) control algorithm. The control and bias coils are driven by a pulse-width-modulated (PWD) amplifier. The controller would attempt to force the journal to a centered position at all times, regardless of load. However, in a loaded foil bearing the journal runs at some eccentricity and attitude angle when supporting a load. One approach to coordinate the characteristics of the two bearings was a supervisory control system [6]. The graphical user interface (GUI) on a PC screen was user friendly,

allowing for easy change of PID parameters, AMB currents and CFB offset values.

All of the output signals from probes near AMB, CFB and REB were connected with the oscilloscopes and the FFT analyzer to show the orbit of the rotor and the corresponding vibration responses. Finally, these signals were recorded on the tape for further analyses.

For data acquisition, two data recording system were employed. A 24 channel 16-bit high speed, digital data acquisition system that samples all channels simultaneously was used in parallel with a 14 channel, analog data recorder to store test results. The system user interface is a custom interface to MATLAB. This user interface developed in MATLAB allowed for real time as well as post-test data analysis. The analog data recorder was used as back-up to the digital data acquisition system as well as to monitor rig performance between test events. The dynamic data with a fast pace reduction rate, such as rotor motion and displacement of all support bearings stations in the X–Y direction as well as the rotor speed, were recorded via a digital Sony tape recorder. All other data, such as temperatures, pressures, static positions, and loads, were recorded via the Lab View program. The parameters recorded by Lab View were interactively observed on the computer screen in the form of plots or numerical values and any sudden changes in the parameters could be discerned. The output data for the Lab View program was a text file that could be read by most ASCII programs. After the numerical data were extracted from Lab View, a plotting program such as Excel or SigmaPlot was used to generate plots. The tape recorder featured a computer program that transferred the recorded signal to a PC in the form of a binary file. A MATLAB program was written, which was able to read the data from the binary file. The MATLAB program then plotted the data based on the recording time or speed of the rotor. Variation of the rotor orbit vector (magnitude plus phase angle) with rotor speed, at a particular axial location, known as “order track” and a 3D “waterfall” drawing showed the relationship among magnitude, rotor speed and elapsed time.

### OPERATIONAL CHARACTERISTICS

The present experimental program was aimed at extending the applicability of foil bearings to larger bearing sizes, higher loads and higher speeds than had been demonstrated previously. In particular, the goal was to do an extensive series of tests in order to verify the performance of the largest  $\phi 150$  mm CFB at different operating conditions. These tests focused on following different modes by means of switching AMB on or off:

- (1). AMB mode at low speed;
- (2). CFB mode at high speed;
- (3). Hybrid mode when AMB is treated as a bearing;
- (4). Hybrid mode when AMB is treated as a loader.

In this experimental investigation a side-by-side configuration was selected. The AMB located in the middle of the rotor and the CFB was as close to AMB as possible.

### ROTOR MODE SHAPE PREDICTION

Prior to dynamic testing, the natural frequencies of the rotor needed to be measured with free-free impact test, as shown in Tab.1.

Tab.1 Natural frequencies of solid shaft using free-free impact test

Mode No.	1	2	3
Free-free impact test	580 Hz	1,516 Hz	2,328 Hz

More accurate analytical model of the DyRoBeS was set up in Fig.4, considering the boundary conditions in the ball bearing set (REB). The first two rigid modes and the third bending mode are shown in Fig.5. Their corresponding critical speeds are 4,019 rpm, 11,062 rpm and 32,438 rpm, respectively.

### ROTOR-BEARING TESTING RESULTS

The rotor was levitated by AMB at zero speed and started to run up in the hybrid HFMB mode in order to evaluate the operation at increasing speeds. A soft-start algorithm of the AMB controller was used to levitate the rotor during start-up and coast-down. This helped to minimize foil bearing coating wear and reduce the start-up torque, since this feature allowed essentially zero-wear operation of the bearing. More importantly, the required low speed/start-up motor torque was reduced significantly, since very little load was carried by the foil bearing at speeds where rubbing would be expected to occur. This feature was especially useful due to torque limitations of the high speed motor used. Upon reaching to the CFB lift-off speed, load sharing between CFB and AMB occurred in hybrid mode. In another test case, when speed was above the CFB lift-off speed (say 4,000 rpm), the AMB was tuned off to let rotor drop down on the CFB in the CFB mode alone and the operation was evaluated. Before running beyond the second critical speed, the dynamic balance of the rotor should be done. In order to improve the CFB stiffness and damping efforts, the alignment between CFB and rotor was verified. A kind of damping material was employed in the REB set. Therefore, the  $\phi 150$  mm CFB testing has traversed through its first (4,019 rpm) and second rigid critical speed (11,062 rpm) and reached to 26,923 rpm (i.e. 4 MDN,  $v=211.45$  m/s). At this speed a 180 kg static radial load was applied to CFB by AMB as a loader. The highest speed lasted for a couple of minutes, a new record for the largest  $\phi 150$  mm foil bearing so far. Unfortunately, in an attempt to go further, when air flow was increased in order to decrease the temperature rise, one of the two supply tubes burst; therefore, suddenly reducing the amount of cooling air. After coast down to a stop and disassembly of the CFB, no problem could be detected. Thus it was concluded that approximately 0.038 kg/s at 12 psig cooling air flow rate is sufficient at the speed and load specified. Additionally, proof was obtained that the Korolon 800 coating contains good anti-wear property. During the test, displacements in X and Y directions at different positions in axial direction, temperatures on the CFB surface at upstream and downstream ends, cooling air flow rate and pressure, applied load by AMB, rotor speed and its orbit have been monitored and recorded.

The run-up/coast-down of rotor is shown in Fig.6. The rotor was levitated by AMB at zero speed and drove to run up in the hybrid HFMB mode until 7,600 rpm. The AMB was then turned off to let CFB work alone and the rotor speed was gradually increase to reach the top speed 26,923 rpm. During the accelerative time period some load was applied with AMB as a loader. The FFT recording was not taken due to an emergency; however, the coast-down FFT response curve taken at 25,125 rpm was recorded and shown in Fig.7. It was noted that the magnitude of the displacement at 25,125 rpm is only 8  $\mu\text{m}$ . A peak signal was caused by switching on the AMB. Fig.8 shows a typical synchronous response of the vertical displacement of CFB for speeds up to the highest of 26,923

rpm. This shows that the magnitude of the displacement of the CFB at 26,923rpm is only 11.4 $\mu$ m. The response curve further shows two very well damped rigid modes at the first critical speed 4,019 rpm and the second critical speed 11,062 rpm. Between them, a peak of about 8,000 rpm was not related to critical speed but to the applied loading from AMB. During run-up and coast-down between 0 rpm and 26,923 rpm (i.e. 4 MDN), maximum amplitudes of rotor vibration did not exceed 20  $\mu$ m even passing through the two rigid shaft modes of the system. Fig.9 shows the corresponding waterfall plot for this test run. The real temperature and the temperature rise between upstream and downstream in CFB versus speed is shown in Figs.10 a and b. Note that the temperature growth is quite stable with the speed increasing and the maximum temperature at 26,923 rpm is a reasonable 60 $^{\circ}$ C. The temperature rise is less than 1 $^{\circ}$ C at most. As shown in Fig.11, the rotor orbit near CFB is stable even at 26,923 rpm.

On the other extreme side, recognizing that many larger gas turbine engine rotor systems operate at speeds below 15,000 rpm, a preliminary evaluation of the bearing's low speed ability was also completed. To determine the minimum shaft operating speed (i.e. touchdown speed) for foil bearing alone operation, the rotor was spun to a speed of approximately 3,000 rpm, and the magnetic bearing turned off so that the rotor's free end was supported solely by the CFB. The drive motor was turned off and the rotor was then allowed to decelerate to rest. As noted in the synchronous peak hold spectrum plot, shown in Fig.12, rotor-to-foil contact and touchdown occurs at only approximately 645 rpm. This extremely low spin speed is equivalent to a surface velocity U of less than 5 m/s. Foil bearing temperatures during the low speed operation were also measured, as shown in Fig.13. Temperatures were very stable, showing only a minor increase during the final stages of shutdown. This increase was due to the short amount of time when the shaft was rubbing on the bearing smooth foil coating.

It is noted in the touchdown speed test that the non-contact operation of  $\phi$ 150 mm CFB was maintained at a speed as low as 645 rpm with rotor weight of 55 kg. Therefore, the bearing load capacity coefficient[1]  $D=W/(LD)/(D\Omega)=120/(5.9*4.0)/(5.9*0.645) = 1.34 > 1.0$ . That means the CFB design of top and bump foil structure is good at trapping and maintaining the air film between the shaft and top foil in order to improve the load capacity. Since AMB is limited to apply more loading on the CFB, another loading device needs to be set up for further investigation of this  $\phi$ 150 mm CFB load capacity at high speed.

As mentioned previously, one of the advantages of the hybrid HFMB is the redundancy in the bearing system. In most applications, this redundancy can eliminate the need for an auxiliary/backup bearing for the magnetic bearing. Two distinct regimes of operation must be considered. The first is failure of AMB at operating speed with a potential requirement for the CFB to act as the primary load support. The second is failure at a lower speed, wherein the CFB would need to provide adequate shaft support for a safe machine shut-down. Note that continued operation will, out of necessity, also require the ability for eventual safe coast-down in most applications. Therefore, besides testing the largest  $\phi$ 150 mm CFB to assess its highest speed (26,923rpm, i.e. 4 MDN so far) and determine the lowest speed (touchdown speed 645 rpm) when the hydrodynamic film can no longer support the rotor load, testing was also accomplished to demonstrate the ability of the foil bearing as an auxiliary/backup bearing to continue to

operate after a simulated failure of the AMB, even at low speeds. The simulated AMB failures were conducted at speeds of 1,200, 1,000, 900, 800 and 700 rpm by means of frequently switching AMB "off" and "on" in turn during the coast down course (see Fig.14). Fig.15 presents a typical vertical rotor displacement response versus time to simulated complete AMB failure, even at a low speed of only 700 rpm. The figure shows steady state operation prior to the simulated failure, the failure drop transient, and the rotor continued to operate on the CFB alone without any evidence of rotor-to-foil bearing contact, either in frequency response (Fig.12) or bearing temperature rise (Fig.13). This testing demonstrated a coast-down to full stop under shaft load without bearing damage. Thus, except possibly in the case of extremely high bearing loads, the foil bearing also provides a safe shut-down capacity.

## CONCLUSIONS AND DISCUSSIONS

From the experimental investigation and the data presented, several key features and conclusions can be made:

1. The development of large, high load capacity CFB is crucial to the development of advanced oil-free gas turbine engine applications. To show that foil bearings have the ability to meet the advanced gas turbine engine needs, a  $\phi$ 150 mm diameter compliant foil journal bearing was designed, fabricated and tested, that is believed to be the largest compliant foil journal bearing ever built and tested. For that goal, an existing test rig was modified. Combined with previous work on CFB, a series of CFB in the range of  $\phi$ 10 mm  $\phi$ 35 mm,  $\phi$ 50 mm,  $\phi$ 100 mm to  $\phi$ 150 mm have been set up, both in design parameters and testing data. It is shown that CFB is capable of operating both in hybrid HFMB mode and CFB alone mode up to 4 MDN and very low lift-off (or touchdown) speed (as low as 5 m/s). Additionally, CFB functioned well as an auxiliary/backup device supporting the transient impact of an AMB shutdown. It proved capable of either supporting the shaft during coast-down or during continued operation.

2. The performance of the largest  $\phi$ 150 mm CFB has been investigated up to 26,923 rpm (i.e. 4 MDN). The tests on this bearing demonstrate the viability of scaling existing foil journal bearing designs to the larger sizes required for an advanced gas turbine application. Different operating modes by means of switching the AMB "on" or "off", have been performed: (a). AMB mode at low speed; (b). CFB mode at high speed; (c). Hybrid mode with AMB as a bearing; (d). Hybrid mode with AMB as a loader; and (e). Simulated AMB failures with CFB as an auxiliary/backup bearing. The experimental investigation strongly proved the hybrid HFMB mode is feasible, reliable and robust for AMB as a bearing in hybrid mode or as a loader in CFB mode alone, as well as with CFB as a bearing in hybrid mode or as an auxiliary/backup bearing for AMB. In addition, the HFMB has greater stability margin than the AMB alone, most likely due to stiffness and damping introduced by the CFB.

3. Maximum speed achieved so far for the  $\phi$ 150 mm foil bearing operating alone has been approximately 27,000 rpm or the equivalent of over 4.0 million DN. At this speed, a 180 kg static radial load was applied and approximately 0.038 kg/s cooling air flow rate at 12 psig is sufficient for this condition. In this instance, the magnetic bearing was used as a static loader instead of a load sharing bearing. Higher static or simulated maneuver loads will be tested to verify the expected high load capacity for this bearing. As

shown in Fig.16 the load capacity for this bearing is projected to exceed 1140 kgs at a speed of 14,000 rpm.

4. Recognizing that many larger gas turbine engine rotor systems operate at speeds below 15,000 rpm, a preliminary evaluation of the bearing's low speed ability was also completed. Low speed testing showed that the  $\phi 150$  mm foil bearing alone continued to support the 55 kg rotor static load without shaft/bearing contact at speeds below 700 rpm. The surface velocity is less than 5 m/s. That means the lift-off speed of this  $\phi 150$  mm foil bearing in hydrodynamic region begins at very low speed.

5. Transient tests, simulating magnetic bearing failures at speeds as low as 700 rpm, were also completed, showing that CFB is capable of being a reliable, high performance, auxiliary/backup bearing for the magnetic bearing system if AMB fails or becomes overloaded.

6. To prevent the rotor and bearing surfaces from the severe rub and wear during the start up and shut down to a stop, Korolon 800 as anti-wear solid film lubricant coating was applied and satisfactory performance was obtained for the room temperature operating conditions.

7. The temperature and temperature rises in the compliant foil bearing are not considered high and the rotor vibration response is in the acceptable range, both at high and low speed. In addition to the bearing load capacity, coefficient  $D$  value shows this foil bearing design is satisfactory. These series of tests proved the application to rotors weighing over 65 kg with compliant foil bearing of the journal diameters in the 150 mm range and have further demonstrated the viability and scalability of the CFB and HFMB designs for application to large rotors, such as are found in intermediate sized aviation gas turbine engines.

8. The above results prove that the CFB is stable over a range of operating speeds both in hybrid mode HFMB and in CFB mode alone and that these advanced foil bearings are capable of meeting the load, stiffness and speed requirements of an advanced gas turbine engine. The follow-up elevated temperature testing is expected to further validate the application potential of this bearing.

#### ACKNOWLEDGMENTS

The authors would like to thank Dr. Mark J. Valco and Dr. Christopher DellaCorte of NASA Glenn Research Center, and Mr. Michael J. Tomaszewski and Mr. James F. Walton II of Mohawk Innovative Technology, Inc. for their insistent support of this work.

#### REFERENCES

- [1] DellaCorte, C., and Valvo, M.J., 2000, "Load Capacity Estimation of Foil Air Journal Bearings for Oil-free Turbomachinery Applications," *Tribology Transactions*, 43(4), pp.795-801.
- [2] DellaCorte, C., Lukaszewicz, M.J., Valvo, K.C. Radil and Heshmat H., 2000, "Performance and Durability of High Temperature Foil Air Bearings for Oil-Free Turbomachinery," *Tribology Transactions*, 43(4), pp.774-780.
- [3] DellaCorte, C., 1998, "A New Foil Air Bearing Test Rig for Use to 700°C and 70,000 rpm," *Tribology Transactions*, 41(3), pp.335-340.

- [4] Heshmat, H.1999, "The Integration of Structural and Fluid Film Dynamic Elements in Foil Bearings Part I: Past Approaches to the Problem," ASME Paper DETC99/VIB-8271.
- [5] Heshmat, H., 1994, "Advancement in the Performance of Aerodynamic Foil Journal Bearing- High Speed and Load Capacity," ASME Journal of Tribology, 116, pp 287-95.
- [6] Heshmat,H.,Chen,H.M., and Walton, J.F., 2000, "On the Performance of Hybrid Foil-Magnetic Bearings ", *Journal of Engineering for Gas Turbines & Power*, 122, pp73-81.
- [7] Hibner, D.,and Rosado, L.,1992, "Feasibility of Magnetic Bearings for Advanced Gas Turbines,"*Proc.International Symp. on Magnetic Suspension Technology, NASACP3152*
- [8] Kirk, R.G.,1997, "Evaluation of AMB Turbomachinery Auxiliary Bearings," ASME Paper No. DETC97/VIB-4059.
- [9] Swanson, E.E, Walton, J.F., and Heshmat, H., 2002, "A Test Stand for Dynamic Characterization of Oil-Free Bearings for Modern Gas Turbine Engines," ASME Paper GT-2002-30005.
- [10] Swanson, E. E, and Heshmat,H.,2002,"Oil-free Foil Bearings as a Reliable, High Performance Backup Bearing for Active Magnetic Bearings," ASME PaperGT-2002-30291.
- [11] Swanson, E. E, Heshmat, H., and Walton, J.F., 2000a, "Performance of a Foil-Magnetic Hybrid Bearing," ASME Paper 2000-GT-0411.
- [12] Swanson, E.E, Walton, J.F., and Heshmat, H. 2000b, "A Gas Turbine Engine Backup Bearing Operating Beyond 2.5 Million DN," ASME Paper 2000-GT-0622.
- [13] Swanson, E.E, Walton, J.F., and Heshmat, H., 1999, "A 35,000 RPM Test Rig for Magnetic, Hybrid and Back-up Bearings," ASME Paper 99-GT-180.
- [14] Salehi M., and Heshemat H., 2001,"High Temperature Magnetic Auxiliary Bearings", AFRL-PR-WP-TR-2001-2114 Final Report.
- [15] Heshmat, and H.,Ku, C-P.R., 1994, "Structural Damping of Self-acting Compliant Foil Journal Bearings," ASME Journal of Tribology, 116, pp 76-82.
- [16] Braun M.J., Choy F.K., Dzodzo M., and Hsu J., 1996, "Steady-State and Transient Dynamic Simulation of a Continuous Foil Bearings," *Tribology Transactions*, 39(2), pp.322-329.
- [17] Suriano, F.J., Dayton, R.D., and Woessner, F.G., 1983, "Test Experience with Turbine-End Foil Bearing Equipped Gas Turbine Engines," ASME Paper No. 83-GT-73.

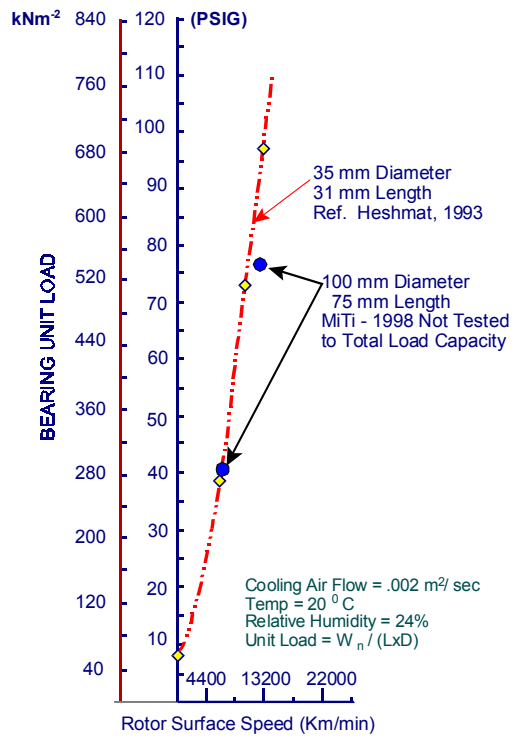


Fig.1 Comparison of load capacity for 35 mm and 100 mm diameter CFBs

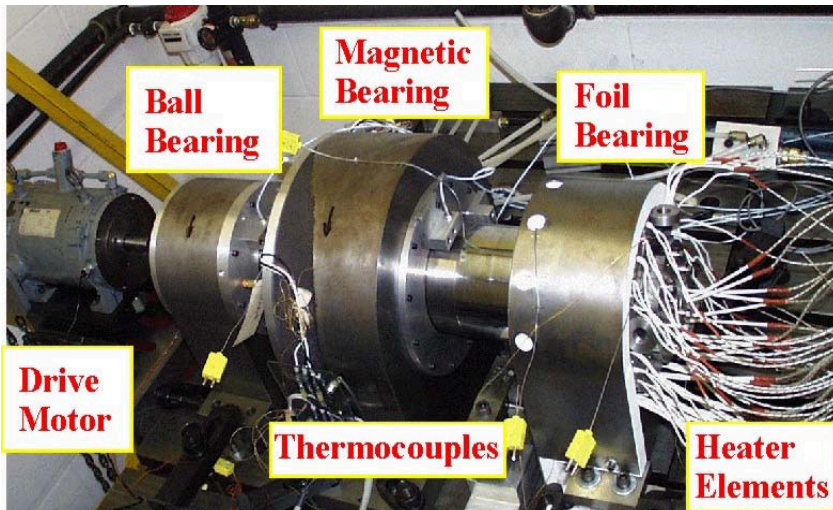


Fig.2 High-speed HFMB test rig set-up



Fig.3 Test rotor and foil journal bearing

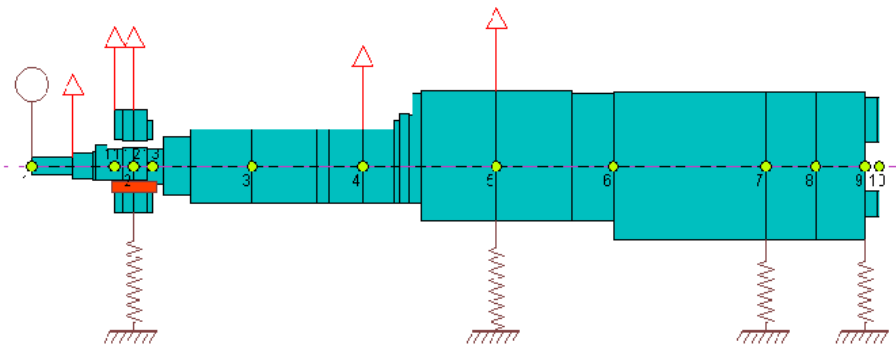
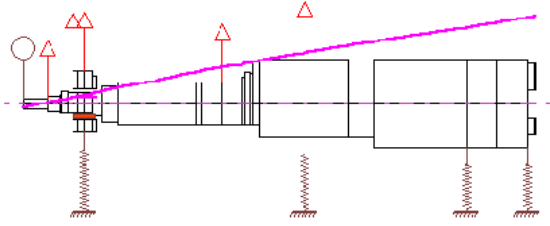


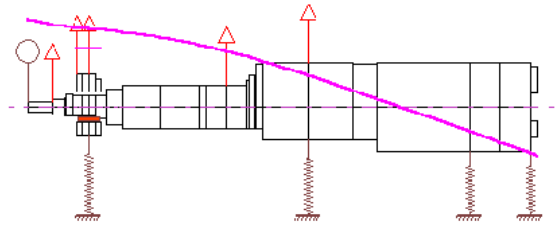
Fig.4 Rotor dynamic analysis model with DyRoBeS

Mode No = 1, Critical Speed = 4019 rpm



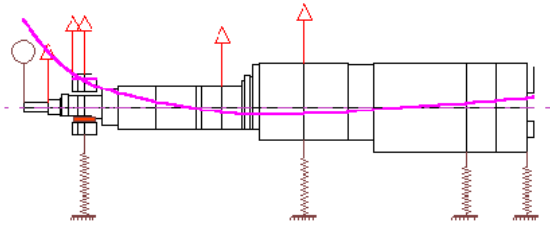
(a) 1st mode 4,019 rpm

Mode No.= 2, Critical Speed = 11062 rpm



(b) 2nd mode 11,062 rpm

Mode No.- 3, Critical Speed = 32438 rpm



(c) 3rd mode 32,438 rpm

Fig. 5 First three mode shapes of the solid shaft

### Shaft RPM vs. Time

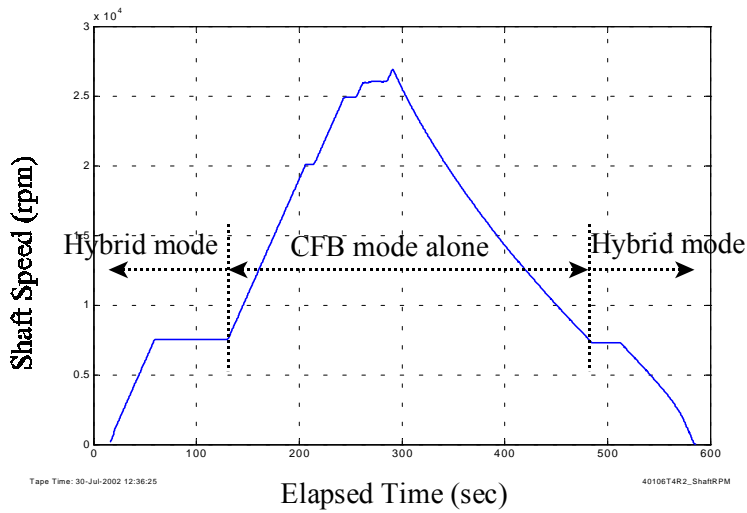
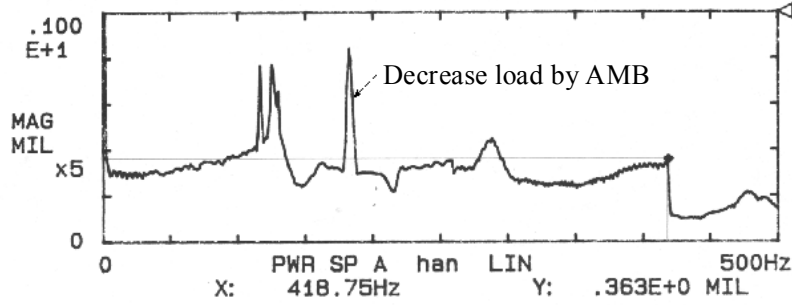
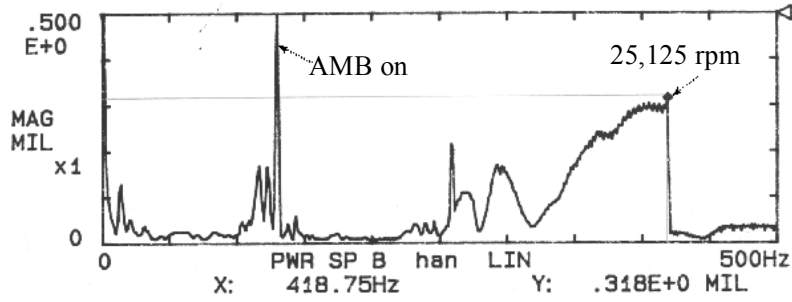


Fig. 6 Shaft speed curve

HFMB T4R1 CHA--HFOIL CHB--VFOIL 07/30/02  
 500Hz A: DC/ 1V B: DC/0.1V S.PEK 769/16 DUAL 1k



30/07/02 09: 31

Fig.7 FFT response of CFB at vertical and horizontal directions respectively

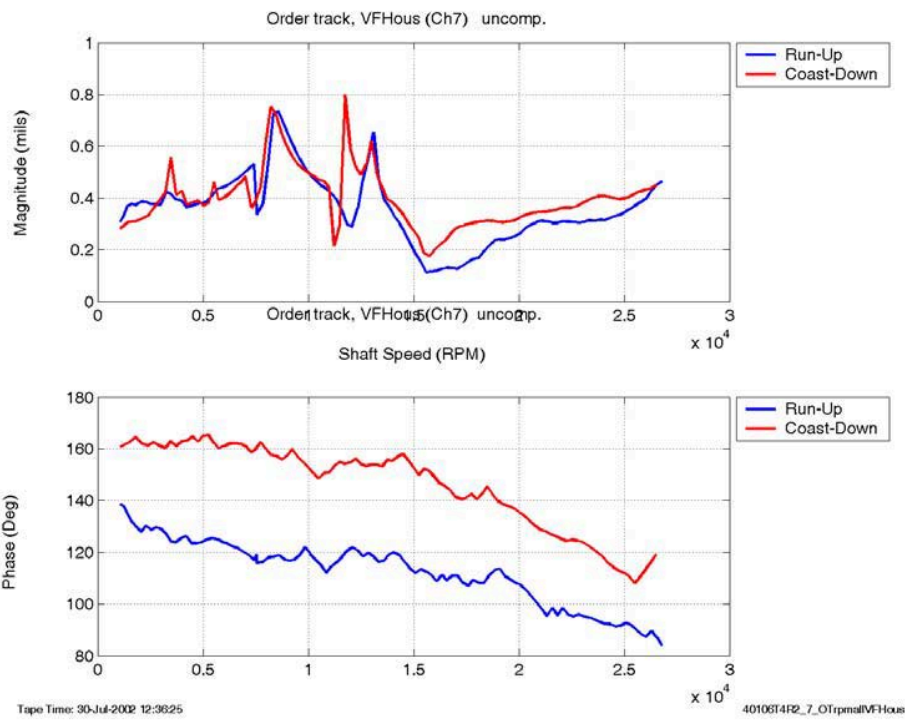


Fig.8 Order track of vertical response of CFB during run-up and coast-down

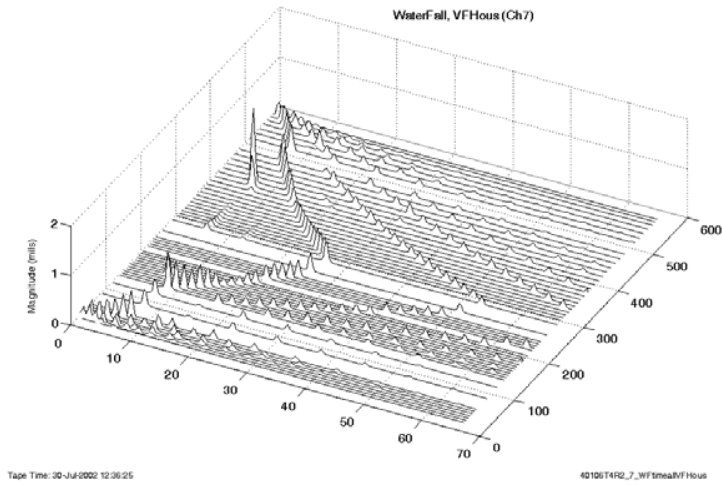


Fig.9 Waterfall of vertical response of CFB

Temp out of foil brg TC4 vs. speed during run-up for  $\phi 5.9''$  (150mm) Foil bearing

Temp rise  $\Delta T$  (=TC4-TC3) vs. speed during run-up for  $\phi 5.9''$  (150mm) Foil bearing

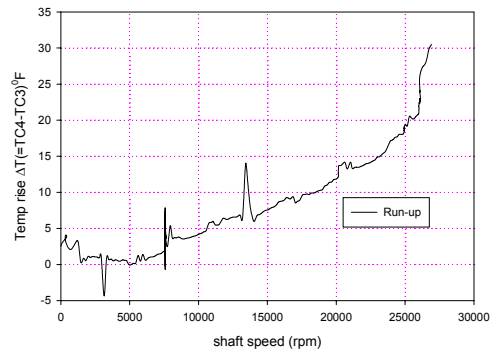
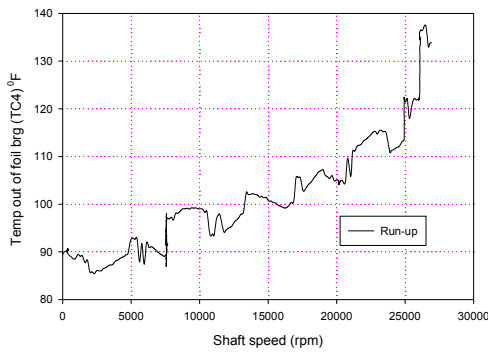
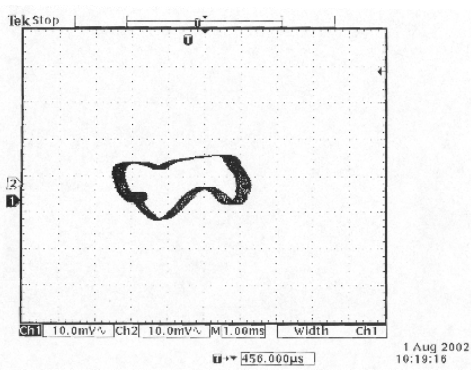
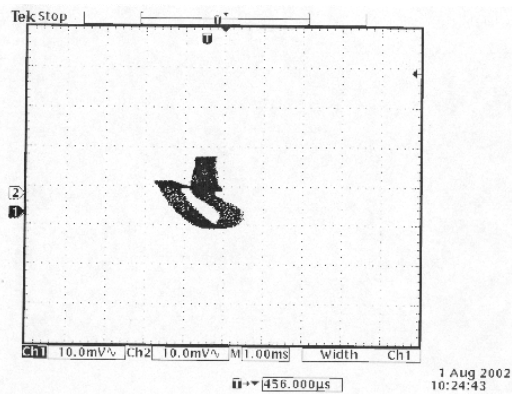


Fig.10 CFB temperature and temperature rise curves



(a). at 7,500 rpm



(b). at 26,923 rpm

Fig.11 Rotor orbits near CFB positions

## Peak Hold, Rotor Coast Down Plot

Coast Down From  $\approx 3,000$  RPM

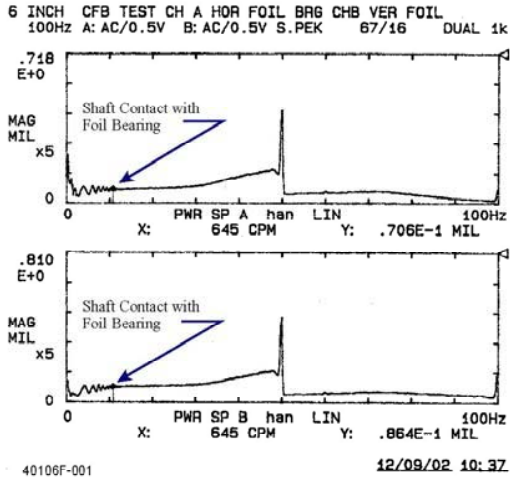


Fig.12 FFT response of CFB at low-speed during touchdown test

## Foil Bearing Temperatures vs Speed

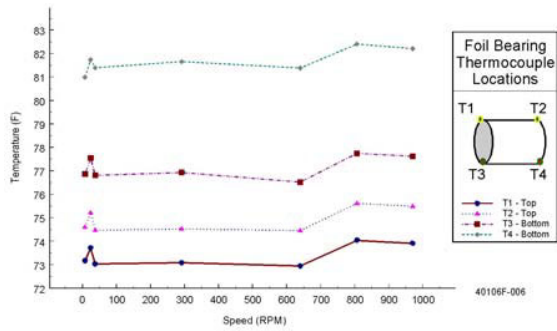


Fig.13 CFB temperature vs. speed during coastdowns

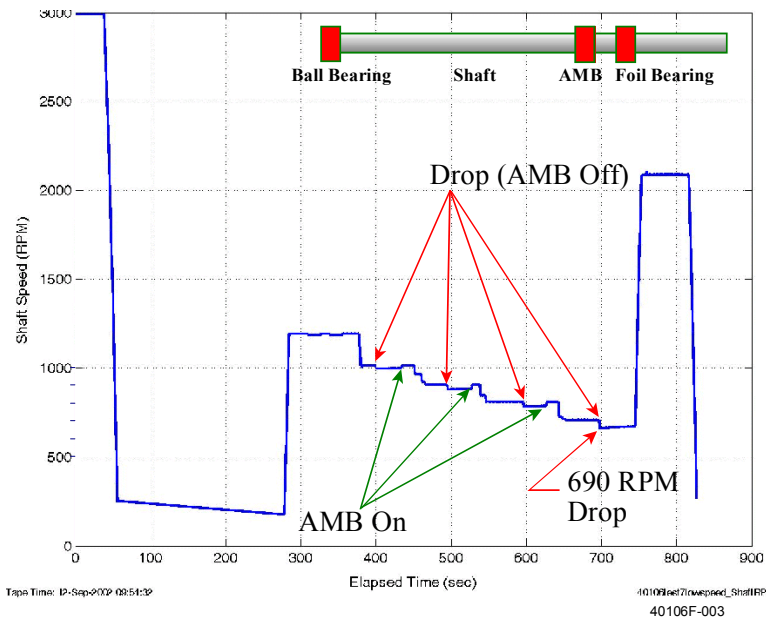


Fig.14 Shaft speed curve at low speed period, shown AMB 'on' and 'off' frequently

40106 HYBRID FOIL MAG 700 RPM DROP 9/12/02  
 200Hz A: DC/0.5V B: AC/ 50V INST 0/16 DUAL 1k

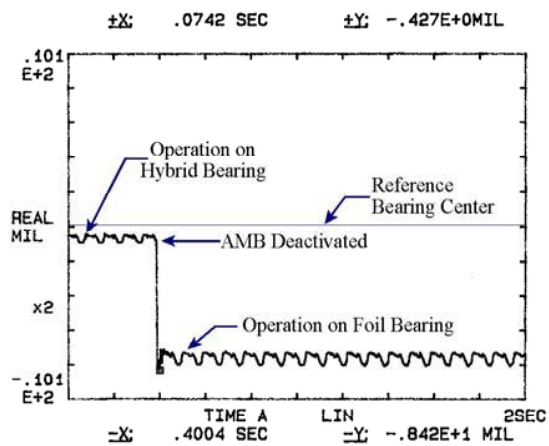


Fig.15 Simulated AMB failure at 700 rpm

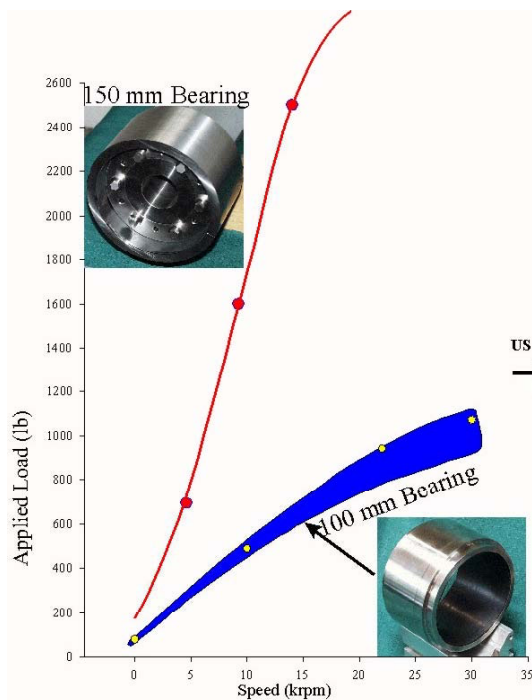


Fig.16 CFB load capacity vs speed